Progress in Energy and Environment

Journal homepage: https://www.akademiabaru.com/submit/index.php/progee/
Link to this article: https://doi.org/10.37934/progee.17.1.116
Special Issue: Sustainable Water Management

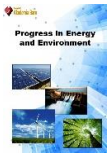

Volume 17 (2021) 1-16

Original Article

The effects of magnetization process on methylene blue removal using magnetically modified orange peel

OPEN ACCESS

Mohamad Huzair Munawer[1], Peck Loo Kiew[*,2], Wei Ming Yeoh[3]

[1] Department of Chemical and Petroleum Engineering, Faculty of Engineering, Technology and Built Environment, UCSI University, 56000 Cheras, Kuala Lumpur, Malaysia
[2] Department of Chemical and Environmental Engineering, Malaysia - Japan International Institute of Technology, Universiti Teknologi Malaysia, Jalan Sultan Yahya Petra, 54100 Kuala Lumpur, Malaysia
[3] Department of Petrochemical Engineering, Universiti Tunku Abdul Rahman, 31900 Kampar, Perak, Malaysia

Abstract

Whilst adsorption process is the preferred method of purifying wastewater due to its benefits, problems with the recovery of spent adsorbents are still prevalent in wastewater treatment technology. The use of magnetized biomass-based adsorbents (biosorbents) to ease the regeneration process would be a novel approach to overcome this obstacle. The magnetization of orange peel adsorbent involves a series of preparation stages. In this context, there are several parameters that may affect the magnetization of orange peel (OP) such as the ratio between $FeCl_3$•$6H_2O$ and $FeCl_2$•$4H_2O$, mass of untreated orange peel (UOP), volume of NH3 solution, magnetization temperature and magnetization period. In this study, Fractional Factorial Design (FFD) was adopted to identify the significant parameters affecting two different responses namely the success of magnetization process and methylene blue (MB) dye removal. Based on the ANoVA results, the significant parameters affecting the success of the magnetization process were magnetization temperature, interaction between ratio of FeCl2:FeCl3 and volume of ammonia, and mass of OP with duration of mixing. Whereas the significant parameters affecting the MB dye removal were all five of the individual parameters, along with the interaction of amount of OP with the other four parameters, interaction between volume of ammonia with duration of mixing and with ratio of $FeCl_2$:$FeCl_3$, interaction between duration of mixing with temperature and ratio of $FeCl_2$:$FeCl_3$, and interaction between temperature and ratio of $FeCl_2$:$FeCl_3$. The highest recorded MB removal was 89.18%, while the lowest recorded MB removal was 38.76%. The regeneration study also showed that magnetized orange peel could be regenerated at least six times without having a significant reduction in adsorption capacity. The major functional groups of magnetized orange peel before adsorption, after adsorption and after regeneration were all similar, indicating that the spent adsorbent could be regenerated.

Article Info

Received 28 April 2021
Received in revised form 19 October 2021
Accepted 25 October 2021
Available online 3 January 2022

Keywords

Methylene blue
Magnetized orange peel
Fractional factorial design
Regeneration
FTIR

1 Introduction

One of the fundamental requirements for life on earth is water, for without it, life is unsustainable. Of the 97 % of water making up the earth, an approximate amount of only 3 % is freshwater [1]. In addition to that, most of the water resources is unsuitable to be used as potable water prior to treatment.

[*] **Corresponding author** plkiew@utm.my ✉

According to Bureau of Reclamation [2] and Khokhar [3], only 0. 5% of the freshwater is easily accessible, with over 30 % of it being used by the industries. Advancement of industrial and agricultural activities have led to an increase in water pollution, leading to an even more scarce supply of easily accessible clean water. Moreover, with overpopulation also on the rise, the world's water resources are in crisis. In this context, the term "crisis" refers to intensified competition for a clean supply of water for domestic usage. The industries usually produce both organic and inorganic pollutants, which have repeated proven to be a problem that necessitates constant monitoring [4]. Dye effluents are the most significant contributor to the water pollution crisis among the various pollutants discovered to be sources of water contamination. Dyes are used in a variety of industries, including paper, plastics, food, cosmetics, textiles, and so on. They endanger the environment and human life even in trace amounts. Due to its vast industrial applications, methylene blue (MB), a highly soluble dark green crystalline powder, is widely used as dye in various industries, with the textile industry ranking the first in terms of dye usage. MB possesses high toxicity and therefore leads to environmental pollution when accumulated in the environment [5].

There are various types of conventional treatment for dye effluents: solvent extraction phytoremediation, oxidation, evaporation, ion exchange to name a few [6]. All have shown to be either expensive, inefficient or pose an environmental threat. Although various techniques have been employed, adsorption remains to be one of the best techniques to treat polluted water [7]. There are numerous literature reviews exploring the utilization of biomass from agricultural waste as potential adsorbents. According to Anastopoulos et al. [8], the use of biosorbents in water treatment technologies are advantageous from several aspects: biodegradability, availability, reusability and complexity. Biosorbents are also known to have many active binding sites on their surface that increase the efficacy of retaining pollutants under certain conditions. However, the adsorption properties are dependent on intrinsic properties of the materials, whereby any modification or functionalization will cause a change in the surface area, pore size distribution and surface functional groups. Hence, the adsorption efficiency will be affected [9].

Whilst adsorption process is the preferred method to purifying wastewater due to its benefits, problems with the recovery of spent adsorbents are still prevalent in wastewater treatment processes. Aside from the abundance of adsorbents, other factors such as efficiency and complexity of adsorbents, as well as the intensity of the recovery and regeneration of spent adsorbents are among the key determinants of the economic feasibility of the process [10]. The conventional recovery processes of spent adsorbents by the means of centrifugation or filtration are either highly energy intensive or involves complex procedures and time consuming. A novel approach to overcome this obstacle would be the utilization of magnetized biomass-based adsorbents (biosorbents) that would ease the regeneration process. Numerous researches have been conducted and the conclusion of most, if not all, reports minimized handling time, cost effectiveness and greatly reduced energy consumption. These include magnetized papaya seeds, magnetized chitosan and magnetized wheat shells [11–13].

As recently reported by Munawer et al. [14], the presence of carboxylate in the orange peel may cause it to bind to MB molecules, promoting MB removal from aqueous solution. Based on a preliminary study performed by Chee [15], magnetized orange peel demonstrated a promising potential to adsorb MB dye from aqueous solution with up to 97.54 % removal. The magnetization of orange peel adsorbent involves a series of preparation stages. There are several parameters that may affect the magnetization of orange peel such as the ratio between $FeCl_3 \bullet 6H_2O$ and $FeCl_2 \bullet 4H_2O$, mass of untreated orange peel (UOP), volume of NH_3 solution, magnetization temperature and magnetization period. However, the significance of these parameters towards the magnetic properties of the magnetized orange peel (MOP) is yet to be explored. The present study therefore suggests the need to identify the magnetization parameters that significantly influence the magnetic properties and adsorption capacity of MOP synthesized. The aim of this study is to eliminate insignificant variables so that a smaller set of process variables affecting the magnetization process can be obtained [16]. From engineering point of view, this is crucial in order to have a better control over the magnetization process that will in turn affect the adsorption performance of the magnetized adsorbent. In addition to this, the feasibility of adopting regenerated magnetized adsorbent is another interesting scope that is being investigated in this study.

2 Methodology and Experimental Set-Up

2.1 Chemicals/Materials

All chemicals used were of analytical grade and were used as received without any further purification. These included isopropyl alcohol (R&M Chemicals), ethanol (Chemiz), sodium chloride (Chemiz), ferum chloride (Chemiz) and ammonia (Chemiz).

2.2 Screening of process variables affecting the magnetization of orange peel and methylene blue removal using fractional factorial design

In the screening of significant magnetization process parameters, five different process parameters: mass of orange peel (OP), volume of ammonia (NH_3), temperature of mixing, duration of mixing, and ratio of $FeCl_2$:$FeCl_3$, were investigated. Fractional Factorial Design (FFD) of Design Expert (Trial version: 19.2020.1.0) was adopted to develop the experimental design. Based on the FFD design, a total of 16 experimental runs were conducted to determine the significant parameters towards the success of the magnetization process and the adsorption performance of magnetized orange peel (MOP). The response variables of the design were designated as the success of the magnetization process (response 1) and the MB removal percentage after the adsorption process (response 2). Table 1 shows the range of all the parameters investigated in this study.

Table 1 Range of values for parameters investigated in this study

Parameter	Unit	Range
Mass of Orange Peel	g	2 - 6
Volume of Ammonia	mL	10 - 30
Temperature	°C	65 - 85
Duration of Mixing	hour	0.5 – 1.5
Ratio of $FeCl_2$:$FeCl_3$	-	1:1 – 1:3

2.3 Preparation of orange peel

The OP was first cut into smaller pieces before washing it with distilled water to remove any dirt particles from the surface [17,18]. The cleansed and cut OP was then oven dried at 60 °C for 24 hours. Subsequently, the dried OP was crushed and sieved to ensure the size of the OP was consistently smaller than 0.5 mm [19–21]. 30 g of OP powder (OPP) was stirred in isopropyl alcohol for 2 rounds: 1st round with 250 mL of isopropyl alcohol for 5 hours, and the 2nd round with another 250 mL of isopropyl alcohol overnight. Then, the wet OP was subjected to stirring with 250 mL of distilled water at room temperature for 30 minutes. The step of washing with distilled water was done at least 3 to 4 times. It was expected that the OPP was then completely bleached and washed [22–24]. Following that, the filtrate was dried again in the oven at 55°C for 24 hours. The OPP was used as the raw material for the magnetization of orange peel adsorbent.

2.4 Magnetization of orange peel adsorbent

The OPP obtained from Section 2.3 was subjected to magnetization process as described by Chee [15]. Generally, $FeCl_3 \cdot 6H_2O$ and $FeCl_2 \cdot 4H_2O$ were mixed at a fixed ratio (according to the FFD experimental design) and dissolved in 200 mL of distilled water. The mixture was vigorously stirred at 85°C until completely dissolved, then the OPP was added in. After 30 mins of stirring OPP with $FeCl_3 \cdot 6H_2O$ and $FeCl_2 \cdot 4H_2O$, it was followed by gradual addition of 30 % NH_3 solution (volume was based on the FFD experimental design). The color of bulk solution changed from orange to black immediately. The stirring was continued for a further duration at the given temperature (both were according to the FFD experimental design) to synthesis the MOP. MOP was washed several times with distilled water and 0.02 mol/L sodium chloride. The sample was then dried and subjected for MB removal process.

2.5 Adsorption of methylene blue

The adsorption process followed the procedures reported by Chee [15]. Based on the results, the optimum adsorption process conditions to achieve the highest MB removal percentage from the aqueous solution were at pH value of 8, ratio of adsorbent to solution of 1:100, temperature of 40 °C, initial MB dye concentration of 100 mg/L, and 40 mins contact time. The MOP was used as adsorbent for MB removal at these process conditions. The MB removal percentage was calculated using Eq. (1):

$$\text{Percentage Removal} = \frac{C_0 - C_e}{C_0} \times 100\% \quad (1)$$

where C_o (mg/L) and C_e (mg/L) represented initial MB dye concentration and MB dye concentration at equilibrium. The concentration of the treated MB dye was determined by using the UV-Visible Spectrophotometer at wavelength 668 nm [15].

2.6 Desorption study

The regeneration study was performed with slight modification of the work reported by Nunes et al. [25] and Hamdaoui et al. [26]. In this study, the spent MOP was stirred in ethanol repeatedly until the solution remains colorless. After repeated rinsing with ethanol, the MOP was first dried before being reused for MB adsorption. To ensure the solid to liquid ratio remained consistent throughout the adsorption and re-adsorption procedure. The magnetism of the regenerated MOP was tested with external magnetic bar and observed visually.

2.7 Characterization of magnetized orange peel

The characterization study was conducted using Fourier-Transform Infrared Spectroscopy (FTIR) to identify the active groups and bonds present on the surfaces of the MOP before and after adsorption, as well as after the regeneration process. The sample used was MOP sample #14 (Table 2). These functional groups were determined by the peak wavenumber, in cm^{-1}, presented in the spectral region in the range from 4000 to 400 cm^{-1}. Each of the functional groups correspond to a certain range of peak values.

3 Results and Discussion

3.1 Magnetization of Orange Peel Based on the FFD Experimental Design

The preparation of all 16 MOP samples was based on the sets of parameters determined through the application of FFD method. Table 2 presents the 16 sets of parameters generated for the experimental work.

It was observed that some samples, specifically sample #1/7/10/16, were brown in color whilst the remaining samples were black in color. Analyzing the set of parameters of these four samples, it can be deduced that the factors affecting the color of the samples were the interacting parameters between the ratio of $FeCl_2$:$FeCl_3$ with volume of ammonia. Fig. 1 shows the difference in color obtained for MOP resulted from different magnetization process parameters.

Similar to the study conducted by Li et al. [27], the notable difference of colors between the samples could be correlated to their magnetic properties. Brown colored samples showed a weaker magnetic strength compared to the black colored samples. Andrade et al. [28] reported that the color of iron oxide was dependent on its chemical composition and this property could be used to determine the purity of the magnetite nanoparticles. Generally, jet black samples were identified as being pure magnetite, whereas the brown samples were mixed with iron oxides. It was deduced that the difference in color was caused by the interaction between two of the five parameters that were volume of NH_3 solution and ratio of $FeCl_2$:$FeCl_3$. All four of the brown colored MOP were mixed with a ratio of 1:3 with 10 mL of ammonia. It can be visibly seen from Fig. 2 and 3 that whilst 100 % of the black colored MOP was attracted to the external magnet (circled in red), a partial amount of the brown colored MOP was found to be not attracted to the external magnet (circled in blue).

Table 2 The experimental design generated by FFD

Run order	Mass of OP (g)	Volume of NH_3 (mL)	Temperature of mixing (°C)	Duration of mixing (hr)	Ratio of $FeCl_2$:$FeCl_3$
1	6	10	85	0.5	3
2	2	30	85	0.5	3
3	6	10	65	0.5	1
4	6	10	85	1.5	1
5	6	30	65	1.5	1
6	2	30	65	0.5	1
7	6	10	65	1.5	3
8	2	10	65	1.5	1
9	2	30	65	1.5	3
10	2	10	85	1.5	3
11	2	10	85	0.5	1
12	2	30	85	1.5	1
13	6	30	65	0.5	3
14	6	30	85	1.5	3
15	6	30	85	0.5	1
16	2	10	65	0.5	3

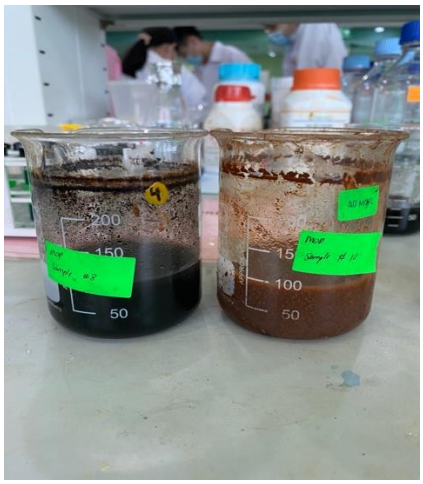

Fig. 1 Black colored MOP (left) and brown colored MOP (right)

3.2 Analysis of Variance of the Success of Magnetization Process

Table 3 is the tabulated results for the success of magnetization process based on the design of experiment generated in FFD, with 3 MOP samples were unsuccessfully magnetized. In this study, the success of magnetization was visually observed through the attraction of the magnetized sample that was dispersed in ammonia solution to the external magnetic bar.

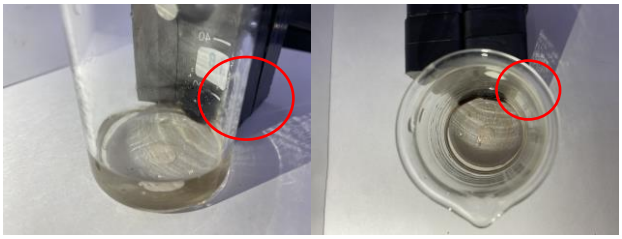

Fig. 2 Black colored MOP

Fig. 3 Brown colored MOP

Table 3 FFD experimental design with the corresponding response variable (success of magnetization)

Run Order	Mass of OP (g)	Volume of NH_3 (mL)	Temperature of mixing (°C)	Duration of mixing (hr)	Ratio of $FeCl_2$:$FeCl_3$	Magnetization
1	6	10	85	0.5	3	0
2	2	30	85	0.5	3	1
3	6	10	65	0.5	1	1
4	6	10	85	1.5	1	1
5	6	30	65	1.5	1	1
6	2	30	65	0.5	1	1
7	6	10	65	1.5	3	0
8	2	10	65	1.5	1	1
9	2	30	65	1.5	3	1
10	2	10	85	1.5	3	1
11	2	10	85	0.5	1	1
12	2	30	85	1.5	1	1
13	6	30	65	0.5	3	1
14	6	30	85	1.5	3	1
15	6	30	85	0.5	1	0
16	2	10	65	0.5	3	1

Note: For "Magnetization"- 0 represents unsuccessful magnetization and 1 represents successful magnetization

Table 4 is the tabulated ANoVA results for the success of magnetization process. The model F-value of 4.00 implied the model was significant. There was only a 4.20 % chance that an F-value this large could occur due to noise. P-value less than 0.05 indicated that the model terms were significant. In this model, the only significant parameters were identified to be D (temperature), AC (interaction between ratio of $FeCl_2$:$FeCl_3$ with volume of NH_3), and BE (interaction between amount of OP with duration of mixing). Values greater than 0.05 indicated that the model terms were insignificant. The adequate

precision was used to measure the signal to noise ratio and was preferably more than 4. The ratio of adequate signal for this response was 6.667, therefore indicating an adequate signal. Hence, it was significant to represent the relationship between the significant parameters and the response variable (magnetization of orange peel) based on the experimental results attained in this study. The R^2 value of the model was 0.8205, an acceptable value as per mentioned by Kiew and Toong [16].

Table 4 ANoVA analysis of FFD for the success of magnetization process

Source	Sum of Squares	DF	Mean Square	F-value	p-value	Status
Model	2.00	8	0.25	4.00	0.0420	Significant
A - Ratio of $FeCl_2$:$FeCl_3$	0.063	1	0.063	1.00	0.3506	
B - Amount of OP	0.063	1	0.063	1.00	0.3506	
C - Volume of NH_3	0.062	1	0.062	1.00	0.3506	
D - Temperature	0.56	1	0.56	9.00	0.0199	
E - Duration of mixing	0.063	1	0.063	1.00	0.3506	
AC	0.56	1	0.56	9.00	0.0199	
BE	0.56	1	0.56	9.00	0.0199	
DE	0.063	1	0.063	1.00	0.3506	
Residual	0.44	7				
Cor Total	2.44	15				
R^2	0.8205					
Adj. R^2	0.6154					
Predicted R^2	0.0623					
Std. Dev.	0.25					
Adeq. Precision	6.667					

Eq. (2) shows the correlation equation, in terms of coded factors, between the response (success of magnetization) with the significant parameters.

$$\text{Success of the magnetization process} = 0.81 - 0.19D + 0.19AC + 0.19BE \quad (2)$$

3.3 Effects of significant parameters affecting the success of the magnetization process

According to Dada et al. [29], temperature is an important factor to be considered when synthesizing magnetic nanoparticles as the temperature of the synthesis controls the reaction kinetics of the process. An increase in temperature leads to an increase in the rate of reaction as the effective collision and the frequency factor of the reacting species are increased. As described by Roonasi and Holmgren [30], the overall reaction to explain the synthesis of magnetite for 2:1 ratio of Fe^{3+} to Fe^{2+} can be written as Eq. (3). At higher temperature, the reaction occurs rapidly with visibly seen magnetite crystals after the addition of ferum chloride mixture into the solution.

$$Fe^{2+} + 2Fe^{3+} + 8OH^- \rightarrow Fe_3O_4 + 4H_2O \quad (3)$$

Aside from temperature, the interaction between the ratio of ferric ions with volume of NH_3 was also a significant factor contributing to the success of the magnetization process in this study. Chen et al. [31] conducted an experiment where the usage of $FeCl_3$ as the treatment solution did not yield ferromagnetic nanoparticles, however, treatment with $FeCl_2$ did. It was suggested that this occurrence was due to the oxidation of Fe^{2+} to Fe^{3+} inducing the magnetic transition. Schwaminger et al. [32] claimed that the higher the ratio of iron salts to the base (NH_3 in this case), the higher the probability of obtaining magnetic nanoparticles. This finding could be explained by the thermodynamic stability of the magnetite phase in an alkaline environment of higher strength. This is further supported by Li et al.

[27] where she concluded the use of a higher volume of NH_3 resulted in a stronger magnetic properties of magnetite nanoparticles.

The last significant parameter affecting the success of the magnetization was the interaction between the amount of OP with the duration of mixing. Dada et al. [29] stated that the contact time and duration of mixing influenced the growth of silver nanoparticles. Additionally, in general, as the duration of mixing increases, more ferric ions will get adsorbed onto the OPP. Alongside the duration of mixing, the amount of OPP determined the number of active sites available [33]. As more OPP is present and longer duration of mixing is allowed, more ferric ions will get adsorbed onto the surface of the OPP, hence explaining the significant interaction between these two variables in affecting the success of MOP magnetization.

3.4 Adsorption performance of magnetized orange peel

Apart from the success of magnetization, the adsorption performance of all the MOP samples synthesized according to the magnetization process parameters specified in Table 3 was investigated based on the adsorption process as described at Section 2.4. Table 5 tabulates the experimental results (average of duplicate results) and predicted MB removal percentage by the FFD.

Table 5 FFD experimental design with the corresponding response variable (MB removal percentage)

Run Order	Absorbance Value			Final Concentration, Ce (mg/L)	MB Removal Percentage (%)	
	1	2	Average		Actual	Predicted
1	1.149	1.092	1.121	23.06	76.94	76.99
2	0.735	0.734	0.735	15.12	84.88	84.83
3	0.745	0.876	0.811	16.69	83.31	83.26
4	1.303	1.044	1.174	24.16	75.84	75.89
5	0.809	0.835	0.822	16.91	83.09	83.14
6	0.990	1.201	1.096	22.55	77.45	77.50
7	0.664	0.516	0.590	12.14	87.86	87.81
8	0.726	0.994	0.860	17.70	82.30	82.25
9	0.623	0.773	0.698	14.36	85.64	85.69
10	0.997	0.909	0.953	19.60	80.40	80.45
11	0.993	0.985	0.989	20.35	79.65	79.70
12	0.647	0.898	0.773	15.91	84.09	84.04
13	1.072	0.988	1.030	21.19	78.81	78.86
14	0.566	0.572	0.569	11.71	88.29	88.24
15	0.508	0.544	0.526	10.82	89.18	89.13
16	1.533	1.443	1.488	61.23	38.76	38.71

Based on the results in Table 5, MOP sample #15 demonstrated the highest MB dye removal percentage, almost as high as the result obtained by Chee [15] under the same adsorption process conditions. However, MOP sample #15 was one of the 3 MOP samples that could not be magnetized (Table 3). The highest MB dye removal percentage performed by a successfully magnetized MOP sample was MOP sample #14 with the removal percentage recorded at 88.29 %.

It was also observed that several of the MOP samples darkened the color of the treated MB dye solution. The cause of this was suspected to be due to dissociation of ferum from the MOP into the solution. Similar pattern was observed from studies conducted by Kalska-Szotsko et al. [34] and Favela-

Camacho et al. [35] where the magnetite nanoparticles changed the color and transparency of the solution.

3.5 Analysis of variance of MB dye removal percentage using magnetized orange peel

Table 6 is the tabulated ANoVA results for the MB adsorption process. The overall model showed a probability value of 0.0138 with R^2 value of 1.000. The model F-value of 3239.09 implied the model was significant with only a 1.38 % chance that an F-value this large could occur due to noise. In this case: Amount of OP (A), volume of NH_3 (B), duration of mixing (C), temperature (D), ratio of $FeCl_2$:$FeCl_3$ (E), interaction between A with B, interaction between A with C, interaction between A with D, interaction between A with E, interaction between B with C, interaction between B with E, interaction between C with D, interaction between C with E, and interaction between D with E, were identified as the significant parameters and interactions. The signal ratio obtained from the model was 245.052 (greater than the ideal value of 4), indicating an adequate signal [16]. Eq. (4) presents the correlation equation between the response variable (MB removal percentage) with the significant parameters in terms of coded factors.

$$\text{MB removal (\%)} = 79.78 + 3.13B + 4.15C + 3.66E + 2.63D - 2.08A - 2.22BC - 2.80BE - 2.98BD + 2.14BA - 2.31CE + 2.56\,CA - 3.91ED + 4.19EA + 2.30DA \quad (4)$$

Table 6 ANoVA analysis of FFD for MB removal percentage

Parameter	Sum of Squares	DF	Mean Square	F-value	p-value	Status
Model	2047.72	14	146.27	3239.09	0.0138	Significant
A - Amount of OP	157.19	1	157.19	3481.00	0.0108	
B - Volume of NH_3	275.31	1	275.31	6095.85	0.082	
C - Duration of mixing	214.11	1	214.11	4741.54	0.0092	
D - Temperature	110.51	1	110.51	2447.34	0.0129	
E - Ratio of $FeCl_2$:$FeCl_3$	69.43	1	69.43	1537.56	0.0162	
AB	78.90	1	78.90	1747.24	0.0152	
AC	125.72	1	125.72	2784.11	0.0121	
AE	142.15	1	142.15	3147.87	0.0113	
AD	73.49	1	73.49	1627.41	0.0158	
BE	85.33	1	85.33	1889.69	0.0146	
BC	104.81	1	104.81	2320.97	0.0132	
CD	244.84	1	244.84	5422.16	0.0086	
CE	281.15	1	281.15	6226.14	0.0081	
DE	84.78	1	84.78	1877.44	0.0147	
Residual	0.0452	1	0.2525			
Cor Total	2047.76	15				
R^2	1.0					
Adjusted R^2	0.9997					
Predicted R^2	0.9944					
Adeq. Precision	245.0520					
Std. Dev.	0.2125					

All five individual parameters; amount of OP (A), volume of NH_3 (B), duration of mixing (C), temperature (D) and ratio of $FeCl_2$:$FeCl_3$ (E), were identified as significant. However, the analysis identified the interaction between C and E as the most significant with the lowest p-value of 0.0081. The predicted data were indicated as a well fitted model with R^2 value of 1.000.

3.6 Effects of significant parameters affecting the adsorption performance of magnetized orange peel

The first significant parameter to affect the MB removal by the MOP was the amount of OP used. Amount of OP was significant both individually and its interaction with the other parameters. In general, the more the amount of OP used, the higher the number of active sites for adsorption of ferric ions [33]. Kheshtzar et al. [36] performed an optimization of reaction parameters for the synthesis of magnetite nanoparticles using pine tree needles through FFD and concluded that the amount of leaf extract used had a significant positive impact on the nanoparticles production. On the other hand, Othman et al. [37] found that a reduction in the maximum adsorption capacities was observed with increasing biosorbent dosage and attributed this occurrence to the overlapping of active sites on the biosorbent.

Volume of NH_3 was the second parameter to have a significant effect on the MB removal. NH_3 affects the pH of the synthesis environment for the magnetization process. In a study done by Setiadi et al. [38] to synthesize magnesium ferrite ($MgFe_2O_4$) based on natural iron sand with various concentrations of NH_3, the authors found that when the NH_3 concentration and density were increased, the size of the nanoparticle crystals decreased. This affected the magnetized nanoparticles' ability to adsorb heavy metal ions and hence impacted the effective contribution to the adsorption process.

Generally, the temperature mainly affects the diffusion of the rate of adsorbate into the pores [16]. This is due to the changes in viscosity of the solution at different temperature. However, it should be noted that an increase in temperature could also lead to an escalated escape tendency of molecules from the adsorbent surface. Maity et al. [39] performed an experiment studying the effects of synthesis temperature and duration of mixing of magnetite nanoparticles. The study concluded that the saturation magnetization increase from 46 to 74 emu/g as the synthesis temperature increase from 220 to 330 °C which could be due to the increase of crystallinity of the particles.

The study by Maity et al. [39] also explained the effects of duration of mixing similarly. The results showed that as the duration of mixing was prolonged from 0.5 to 4.0 hrs, the saturation magnetization also increased from 57 to 65 emu/g. Another possible explanation for the effects these two parameters would be the increase of the particle size as the temperature and/or reaction time is increased. The effects of the particle size are explained in the following paragraph under the effects of ferric ions ratio.

As for the ratio of $FeCl_2$:$FeCl_3$, ferric ions molar ratio affects the particle size and the crystallinity of the ferric nanoparticles [40]. A study conducted by Mizutani et al. [41] showed that the lower the molar ratio between $FeCl_2$:$FeCl_3$ the smaller the particle size and lower crystallinity of the nanoparticles. The particle size directly affected the maximum adsorption capacity of the magnetic nanoparticles. As also mentioned by Hou et al. [42], a smaller particle size equated to more adsorption sites and larger pore volume, hence higher maximum adsorption capacity.

3.7 Regeneration of spent magnetized orange peel

Upon regeneration, the MOP was subjected to MB adsorption process again and the feasibility of regeneration (based on sample #14) is recorded in Table 7 and illustrated in Fig. 4.

Based on the desorption and re-adsorption results, it was observed that the MOP could be regenerated numerous times to be reused for adsorption, with only a deviation of approximately 3 % in between regeneration which is an acceptable range for the regeneration study. The regeneration study was only able to go up to 6 rounds due to major loss of the MOP sample. According to Hassan et al. [43], only a few studies have been conducted to study the possibilities of regenerating magnetic biosorbents, with almost all of these studies reported consistent results with the possibility of regenerating the used magnetic biosorbents up to 3 to 7 times prior to experiencing a significant reduction in adsorption performance. It is also worth to highlight that the magnetic properties of the regenerated MOP did not display any deterioration after undergoing regeneration in this study. The results obtained were sufficient to conclude that MOP was able to undergo regeneration without any significant reduction in its adsorption capacity or magnetic strength.

Table 7 Regeneration of MOP sample #14

Adsorption run order	Absorbance value	Percentage removal (%)
1	0.569	88.29
2	0.615	87.35
3	0.632	87.00
4	0.585	87.93
5	0.486	90.00
6	0.674	86.13

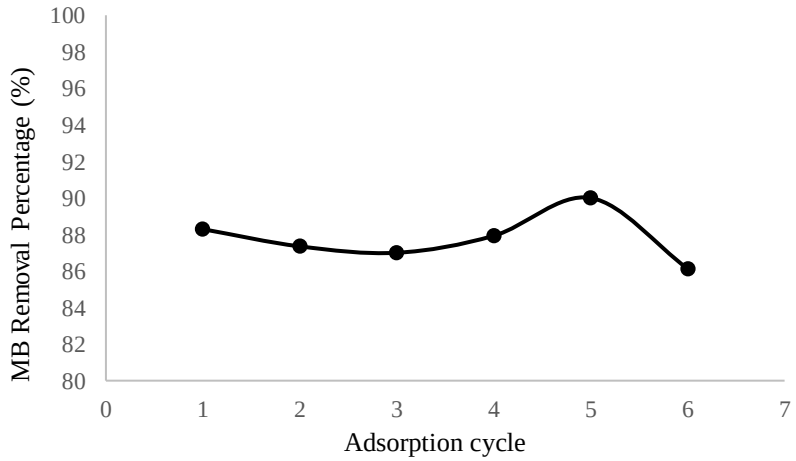

Fig. 4 Regeneration of MOP #14

3.8 Characterization of magnetized orange peel

Three different samples namely the MOP before adsorption, MOP after adsorption, and MOP after regeneration, were subjected to FTIR analysis to identify the major functional groups present in the samples. Fig. 5, 6 and 7 is the illustration of the FTIR spectrum of each sample respectively. As can be seen in all three of the figures, there are a number of adsorption peaks between the 4000-400 cm^{-1} spectral region, indicating the presence of multiple functional groups that define the affinity of the dye molecules to be adsorbed onto or desorbed from the surface of the MOP [44].

Comparing Fig. 5 to 7, it can be seen that the FTIR spectrum for the MOP after adsorption has a high similarity to both the FTIR spectrum of MOP before adsorption and MOP after regeneration. Liu et al. [45], Huang et al. [46] and Chee [15] all reported the significance of the carboxyl groups -COOH, C-O stretching, and O-H to binding with the MB dye molecules. The presence of functional groups before regeneration and after regeneration are very similar, further justifying the feasibility of regenerating the spent MOP. There is a noticeable change in the intensities of FTIR spectrum obtained after methylene blue adsorption, but no change in band position. Similar to the trend observed by Ainane et al. [47], the current results could be also suggesting inclusion of methylene blue with functional groups present in the MOP (mechanical entrapment).

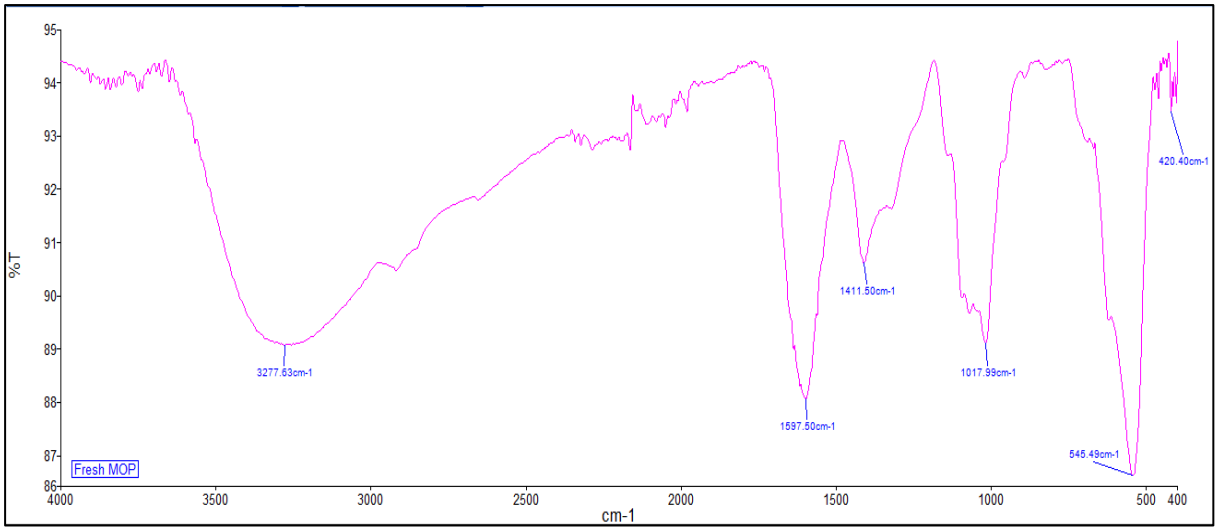

Fig. 5 FTIR spectrum of MOP before adsorption

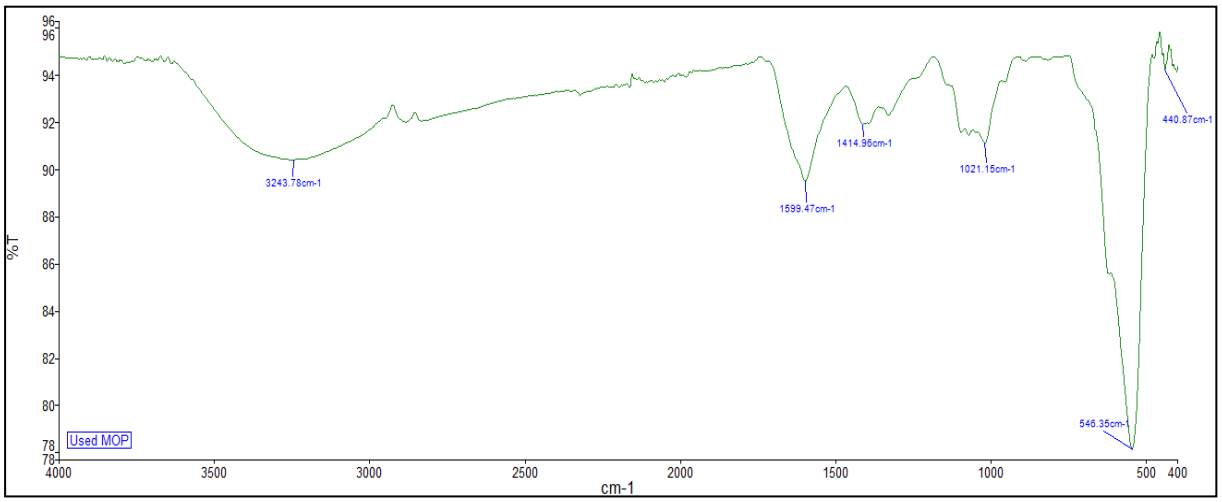

Fig. 6 FTIR spectrum of MOP after adsorption

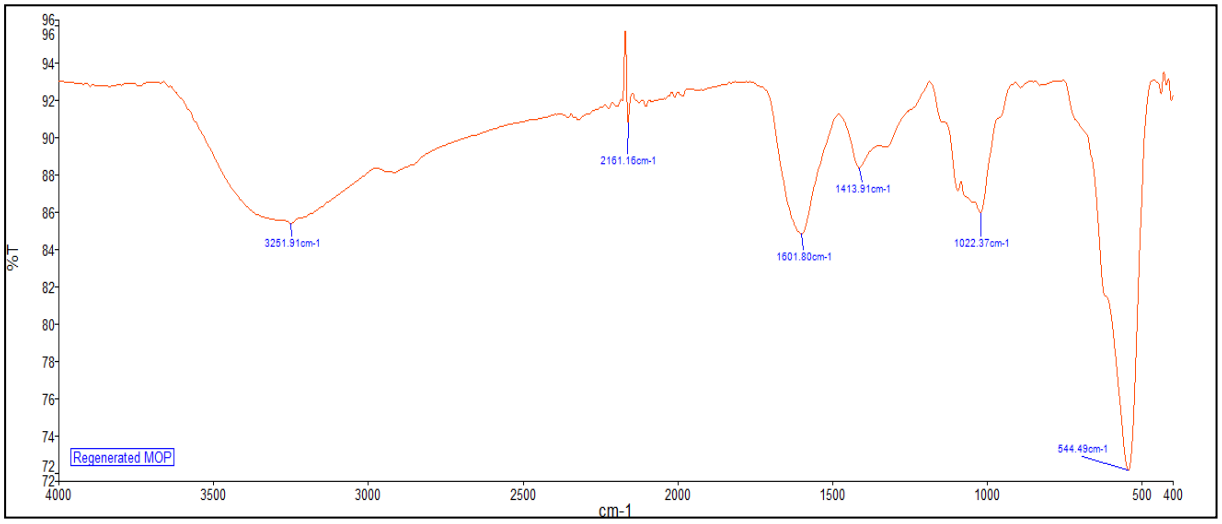

Fig. 7 FTIR spectrum of MOP after regeneration

Overall, there were seven major functional groups detected from the FTIR spectra. These included O-H stretching, C≡C stretching, C=O stretching, C-H bending, N-O stretching, C-O stretching, and C-C stretching. Based on the research by Mohd Nor et al. [48], the wave number of 3243.76 – 3277.63 cm^{-1} could be caused by the presence of alcohol and phenol functional groups, hence the O-H stretching. Whereas the same research suggested the wave number 1597.50 – 1599.47 cm^{-1} could be contributed by the functional group alkene. Boumediene et al. [49] suggested that the wave number 1411.50 – 1413.91 cm^{-1} was associated with aliphatic and aromatic groups. The wave number 700 – 400 cm^{-1}, according to Yang et al. [50], was mostly associated with functional group alkane. However, referring to Fig. 7, there is a distinct peak at wavelength 2161.16 cm^{-1} that could be related to the presence of N=N=N stretching [51]. Based on the chemicals involved and the pre-existing functional groups on the MOP, this anomaly can only be explained by the presence of impurity during the handling of sample for the FTIR analysis. Table 8 correlates the peaks to their respective functional groups.

Table 8 FTIR spectra peak locations and assignment of MOP before/after adsorption and MOP after regeneration [48, 50, 51]

	Peak wave number (cm^{-1})		
Functional groups	MOP before adsorption	MOP after adsorption	MOP after regeneration
O-H stretching	3277.63	3243.76	3251.91
C=O stretching	1597.50	1599.47	-
C-H bending	1411.50	1414.96	1413.91
N-O stretching	-	-	1501.80
C-O stretching	1017.99	1021.15	1022.37
C-C stretching	545.49	546.35	544.49

4 Conclusion

In this study, the effects of various magnetization process parameters on the success of orange peel magnetization and its adsorption performance were investigated using FFD approach. It was observed that that several sets of parameters produced brown colored MOP with weaker magnetic properties compared to the black colored MOP. Based on the ANoVA results, all the parameters included the mass of OP, volume of NH_3, temperature of mixing, duration of mixing and ratio of Fe ions affected the magnetization and MB removal percentage significantly, either individually or interaction with each other. The regeneration study showed that the spent MOP could be regenerated at least 6 times without experiencing any reduction in its adsorption capacity. A deviation of only 3 % was shown throughout the 6 regeneration cycles. The minor differences in IR spectra region of the MOP before adsorption and after regeneration showed the success of the regeneration process. The functional groups of carboxyl and hydroxyl groups contained in the MOP were claimed to be effective constituents for ion exchange with the dye molecules and thus favored the adsorption process.

Acknowledgement

This work is financially supported by the UCSI University Research Excellence & Innovation Grant (REIG) with the grant no. REIG-FETBE-2020/019.

Declaration of Conflict of Interest

The authors declared that there is no conflict of interest with any other party on the publication of the current work.

ORCID

Peck Loo Kiew https://orcid.org/0000-0001-5051-9909

References

[1] USGS, How much water is there on, in, and above the Earth? (2016) Retrieved from http://water.usgs.gov/edu/earthhowmuch.html.
[2] Bureau of Reclamation, Water facts–Worldwide water supply (2020) Retrieved from https://www.usbr.gov/mp/arwec/water-facts-ww-water-sup.html.
[3] T. Khokhar, Chart: Globally, 70% of freshwater is used for agriculture (2017) Retrieved from https://blogs.worldbank.org/opendata/chart-globally-70-freshwater-used-agriculture.
[4] I. Anastopoulos, G. Z. Kyzas, Agricultural peels for dye adsorption: A review of recent literature. Journal of Molecular Liquids, 200 (2014) 381–389. https://doi.org/10.1016/j.molliq.2014.11.006.
[5] M. Hassanpour, H. Safardoust-Hojaghan, M. Salavati-Niasary, 2017. Degradation of methylene blue and Rhodamine B as water pollutants via green synthesized Co_3O_4/ZnO nanocomposite. Journal of Molecular Liquids, 229 (2017) 293–299. https://doi.org/10.1016/j.molliq.2016.12.090.
[6] G. Crini, E. Lichtfouse, Advantages and disadvantages of techniques used for wastewater treatment. Environmental Chemistry Letters, 17 (2019) 145–155. https://doi.org/10.1007/s10311-018-0785-9.
[7] A. Abbas, S. Murtaza, M. Munir, T. Zahid, N. Abbas, A. Mushtaq, Removal of congo red from aqueous solutions with *Raphanus sativus* peels and activated carbon: A comparative study American-Eurasian. Journal of Agriculture & Environmental Science, 10(5) (2011) 802–809. https://www.semanticscholar.org/paper/Removal-of-Congo-Red-from-aqueous-solutions-with-a-Abbas-Murtaza/477a5ab65acedc56665eaac2b41bb069f6808963.
[8] I. Anastopoulos, I. Pashalidis, A. Hosseini-Bandegharaei, D. A. Giannakoudakis, A. Robalds, M. Usman, L. B. Escudero, Y. Zhou, J. C. Colmenares, A. Nunez-Delgado, E. C. Lima, Agricultural biomass/waste as adsorbents for toxic metal decontamination of aqueous solutions. Journal of Molecular Liquids, 295 (2019) 111684. https://doi.org/10.1016/j.molliq.2019.111684.
[9] S. Daneshfozoun, M. A. Abdullah, B. Abdullah, Preparation and characterization of magnetic biosorbent based on oil palm empty fruit bunch fibers, cellulose and ceiba pentandra for heavy metal ions removal. Industrial Crops & Products, 105 (2017) 93–103. https://doi.org/10.1016/j.indcrop.2017.05.011.
[10] M. O. Omorogie, J. O. Babalola, E. I. Unuabonah, Regeneration strategies for spent solid matrices used in adsorption of organic pollutants from surface water: A critical review. Desalination and Water Treatment, 57(2) (2014) 518–544. https://doi.org/10.1080/19443994.2014.967726.
[11] Y. Bulut, H. Aydin, A kinetics and thermodynamics study of methylene blue adsorption on wheat shells. Desalination, 194(1–3) (2006) 259–267. https://doi.org/10.1016/j.desal.2005.10.032.
[12] H. Karaer, I. Kaya, Synthesis, characterization of magnetic chitosan/active charcoal composite and using at the adsorption of methylene blue and reactive blue4. Microporous and Mesoporous Materials, 232 (2016) 26–38. https://doi.org/10.1016/j.micromeso.2016.06.006.
[13] T. S. Jong, C. Y. Yoo, P. L. Kiew, Feasibility study of methylene blue adsorption using magnetized papaya seeds. Progress in Energy and Environment, 14 (2020) 1–12. https://www.akademiabaru.com/submit/index.php/progee/article/view/909/2731.
[14] M. H. Munawer, H. L. Chee, P. L. Kiew, Magnetized orange peel: A realistic approach for methylene blue removal. Materials Today: Proceedings (2021). https://doi.org/10.1016/j.matpr.2021.02.796.
[15] H. L. Chee, Comparative study of methylene blue removal using magnetic modified, chemically treated and untreated orange peel: Adsorption and kinetic studies. [Unpublished bachelor's thesis]. UCSI University (2017).
[16] P. L. Kiew, J. F. Toong, Screening of significant parameters affecting Zn (II) adsorption by chemically treated watermelon rind. Progress in Energy Environment, 6 (2018) 19–32. https://www.akademiabaru.com/submit/index.php/progee/article/view/1048/40.
[17] N. C. Feng, X. Y. Guo, S. Liang, Enhanced Cu (II) adsorption by orange peel modified with sodium hydroxide-TNMSC. The Chinese Journal of Nonferrous Metals, 20(1) (2009) s146–s152. http://www.ysxbcn.com/down/upfile/soft/201076/29-p146.pdf.
[18] K. Y. Foo, B. H. Hameed, Preparation, characterization and evaluation of adsorptive properties of orange peel based activated carbon via microwave induced K_2CO_3 activation. Bioresource Technology, 104 (2012) 679–686. https://doi.org/10.1016/j.biortech.2011.10.005.
[19] M. Arami, N. Y. Limaee, N. M. Mahmoodi, N. S. Tabrizi, Removal of dyes from colored textile wastewater by orange peel adsorbent: Equilibrium and kinetic studies. Journal of Colloid and Interface Science, 288(2) (2005) 371–376. https://doi.org/10.1016/j.jcis.2005.03.020.
[20] N. Feng, X. Guo, S. Liang, Adsorption study of copper (II) by chemically modified orange peel. Journal of Hazardous Materials, 164 (2–3) (2009) 1286–1292. https://doi.org/10.1016/j.jhazmat.2008.09.096.

[21] A. E. Nemr, O. Abdelwahab, A. El-Sikaily, A. Khaled, Removal of direct blue-86 from aqueous solution by new activated carbon developed from orange peel. Journal of Hazardous Materials, 161(1) (2009) 102–110. https://doi.org/10.1016/j.jhazmat.2008.03.060.

[22] X. Li, Y. Tang, X. Cao, D. Lu, F. Luo, W. Shao, Preparation and evaluation of orange peel cellulose adsorbents for effective removal of cadmium, zinc, cobalt and nickel. Colloids and Surfaces A: Physicochemical and Engineering Aspects, 317(1–3) (2008) 512–521. https://doi.org/10.1016/j.colsurfa.2007.11.031.

[23] D. Lu, Q. Cao, X. Li, X. Cao, F. Luo, W. Shao, Kinetics and equilibrium of Cu(II) adsorption onto chemically modified orange peel cellulose biosorbents. Hydrometallurgy, 95 (2009) 145–152. https://doi.org/10.1016/j.hydromet.2008.05.008.

[24] V. K. Gupta, A. Nayak, Cadmium removal and recovery from aqueous solutions by novel adsorbents prepared from orange peel and Fe_2O_3 nanoparticles. Chemical Engineering Journal, 180 (2012) 81–90. https://doi.org/10.1016/j.cej.2011.11.006.

[25] K. G. P. Nunes, L. W. Sfreddo, M. Rosset, L. A. Fèris, Efficiency evaluation of thermal, ultrasound and solvent techniques in activated carbon regeneration. Environmental Technology, (2020) 1–23. https://doi.org/10.1080/09593330.2020.1746839.

[26] O. Hamdaoui, E. Naffrehoux, L. Tifouti, C. Petrier, Effects of ultrasound on adsorption–desorption of p-chlorophenol on granular activated carbon. Ultrasonics Sonochemistry, 10 (2003) 109–114. https://doi.org/10.1016/s1350-4177(02)00137-2.

[27] J. L. Li, D. C. Li, S. L. Zhang, H. C. Cui, Z. Wang, Analysis of the factors affecting the magnetic characteristics of nano-Fe_3O_4 particles. Materials Science, 56 (2011) 803–810. https://doi.org/10.1007/s11434-010-4126-z.

[28] A. L. Andrade, D. M. Souza, M. C. Pereira, J. D. Fabris, R. Z. Domingues, pH effect on the synthesis of magnetite nanoparticles by the chemical reduction-precipitation method. Química Nova, 33(3) (2010) 524–527. https://doi.org/10.1590/S0100-40422010000300006.

[29] A. O. Dada, F. A. Adekola, O. S. Adeyemi, O. M. Bello, A. C. Oluwaseun, O. J. Awakan, F. A. Grace, Exploring the effect of operational factors and characterization imperative to the synthesis of silver nanoparticles. In Silver nanoparticles – Fabrication, characterization and applications, K. Maaz (Ed), Intechopen (2018). https://www.intechopen.com/chapters/61862.

[30] P. Roonasi, A. Holmgren, A study on the mechanism of magnetite formation based on iron isotope fractionation. (2009) Retrieved from https://www.diva-portal.org/smash/get/diva2:1010902/FULLTEXT01.pdf.

[31] Y. Chen, Q. Chen, H. Mao, Y. Lin, J. Li, Preparation of magnetic nanoparticles via a chemically induced transition: Presence/Absence of magnetic transition on the treatment solution used. Journal of Chemistry, 9 (2016). https://doi.org/10.1155/2016/7604748.

[32] S. P. Schwaminger, C. Syhr, S. Berensmeier, Controlled synthesis of magnetic iron oxide nanoparticles: Magnetite or Maghemite? Crystals, 10(3) (2020) 214. https://doi.org/10.3390/cryst10030214.

[33] H. Panda, N. Tiadi, M. Mohanty, C. R. Mohanty, Studies on adsorption behavior of an industrial waste for removal of chromium from aqueous solution. South African Journal of Chemical Engineering, 23 (2017) 132–138. https://doi.org/10.1016/j.sajce.2017.05.002.

[34] B. Kalska-Szotsko, U. Wykowska, K. Piekut, D. Satula, Stability of Fe_3O_4 nanoparticles in various model solutions. Colloids and Surfaces A: Physicochemical and Engineering Aspects, 450 (2014) 15–24. https://doi.org/10.1016/j.colsurfa.2014.03.002.

[35] S. E. Favela-Camacho, J. F. Pérez-Robles, P. E. Garciá-Casillas, A. Godinez-Garcia, Stability of magnetite nanoparticles with different coatings in a simulated blood plasma. Journal of Nanoparticle Research, 18 (2016) 176. https://doi.org/10.1007/s11051-016-3482-2.

[36] R. Kheshtzar, A. Berenjian, S. M. Taghizadeh, Y. Ghasemi, A. G. Asad, A. Ebrahiminezhad, Optimization of reaction parameters for the green synthesis of zero valent iron nanoparticles using pine tree needles. Green Processing and Synthesis, 8(1) (2019) 846–855. https://doi.org/10.1515/gps-2019-0055.

[37] N. Othman, A. S. Che-Azhar, A. Suhaimi, Zinc removal using honey dew rind. Applied Mechanics and Materials, 680 (2014) 150–153. https://doi.org/10.4028/www.scientific.net/AMM.680.150.

[38] E. A. Setiadi, N. S. Asri, Y. A. Wijayanti, A. P. Tetuko, P. Sebayang, P., The effect of ammonia solution concentration on the synthesis process of $MgFe_2O_4$ based on natural iron sand as adsorbent of Pb ions. AIP Conference Proceedings, 2256 (2020) 030011. https://doi.org/10.1063/5.0015497.

[39] D. Maity, J. Ding, J. M. Xue, Synthesis of magnetite nanoparticles by thermal decomposition: Time, temperature, surfactant and solvent effects. World Scientific Publishing Company, 1(3) (2008) 189–193. https://doi.org/10.1142/S1793604708000381.

[40] S. Yean, L. Cong, C. T. Yavuz, J. T. Mayo, W. W. Yu, A. T. Kan, V. T. Colvin, M. B. Tomson, Effect of magnetite particle size on adsorption and desorption of arsenite and arsenate. Journal of Materials Research, 20(12) (2005) 3255–3264. https://doi.org/10.1557/jmr.2005.0403.
[41] N. Mizutani, T. Iwasaki, S. Watano, T. Yanagida, H. Tanaka, T. Kawai, Effect of ferrous/ferric ions molar ratio on reaction mechanism for hydrothermal synthesis of magnetite nanoparticles. Bulletin of Materials Science, 31(5) (2008) 713–717. https://doi.org/10.1007/s12034-008-0112-3.
[42] L. Hou, Q. Liang, F. Wang, Mechanisms that control the adsorption-desorption behavior of phosphate on magnetite nanoparticles: The role of particle size and surface chemistry characteristics. Royal Society of Chemistry, 10 (2020) 2378–2388. https://doi.org/10.1039/C9RA08517C.
[43] M. Hassan, R. Naidu, J. Du, Y. Liu, F. Qi, Critical review of magnetic biosorbents: their preparation, application, and regeneration for wastewater treatment. Science of the Total Environment, 702 (2019) 134893. https://doi.org/10.1016/j.scitotenv.2019.134893.
[44] P. Verma, S. K. Samanta, A direct method to determine the adsorbed dyes on adsorbent via processing of diffuse reflectance spectroscopy data. Materials Research Express, 6 (2019) 015505. https://doi.org/10.1088/2053-1591/aae3f2.
[45] L. Liu, Z. Gao, X. Su, X. Chen, L. Jiang, J. Yao, Adsorption removal of dyes from single and binary solutions using a cellulose-based bioadsorbents. ACS Sustainable Chemistry and Engineering, 3(3) (2015) 432–442. https://doi.org/10.1021/sc500848m.
[46] W. Huang, Y. Hu, Y. Li, Y. Zhou, D. Niu, Z. Lei, Z. Zhang, Citric acid-crosslinked β-cyclodextrin for simultaneous removal of bisphenol A, methylene blue and copper: The roles of cavity and surface functional groups. Journal of the Taiwan Institute of Chemical Engineers, 82 (2018) 189–197. https://doi.org/10.1016/j.jtice.2017.11.021.
[47] T. Ainane, K. Fatima, M. Talbi, M. Elkouali, A novel bio-adsorbent of mint waste for dyes remediation in aqueous environments: Study and modeling of isotherms for removal of Methylene Blue. Oriental Journal of Chemistry, 30(3) (2014) 1183–1189. http://dx.doi.org/10.13005/ojc/300332.
[48] A. Mohd Nor, T. Hadibarata, Z. Yusop, Z. Mat Lazim, Removal of brilliant green and procionred dyes from aqueous solutionby adsorption using selected agricultural wastes. Jurnal Teknologi, 74(11) (2015) 117–122. https://doi.org/10.11113/jt.v74.4880.
[49] M. Boumediene, H. Benaïssa, B. George, S. Molina, A. Merlin, Characterization of two cellulosic waste materials (orange and almond peels) and their use for the removal of methylene blue from aqueous solutions. Maderas. Ciencia y tecnología, 17(1) (2015) 69–84. http://dx.doi.org/10.4067/S0718-221X2015005000008.
[50] S. T. Yang, S. Chen, Y. Chang, A. Cao, Y. Liu, F. Wang, Removal of methylene blue from aqueous solution by graphene oxide. Journal of Colloid and Interface Science, (2011) 24–29. https://doi.org/10.1016/j.jcis.2011.02.064.
[51] Chemistry LibreTexts, Infrared Spectroscopy Absorption Table (2020). Retrieved from https://chem.libretexts.org/@go/page/22645.